PROCEEDINGS OF SCIENCE

X-ray Spectral Properties of the Black Hole Candidates in the Low/hard State

Kazutaka Yamaoka*, **Takehiro G. Miyakawa, Koji Saito, Masami Uzawa, Mariko Arai, Hiroyuki Sakamoto, Tohru Yamazaki, and Atsumasa Yoshida**

Department of Physics and Mathematics, Aoyama Gakuin University, Fuchinobe 5-10-1, Sagamihara, Kanagawa 229-8558, Japan

E-mail: yamaoka@phys.aoyama.ac.jp

We carried out the systematic spectral analysis for 11 black hole candidates (BHCs) in the low/hard state, using archival RXTE and Beppo-SAX data with the energy coverage of 2-250 keV. For in total 301 observations, the simple analytic model, i.e. power-law with an exponential cutoff modified with a smeared edge model, was adopted. Consequently, we found that the photon index is distributed over 1.2–1.8, and the high energy cutoff was more than 40 keV. We also found a clear anti-correlation between the luminosity and the high energy cutoff when the luminosity is larger than 2×10^{37} erg s^{-1}. In addition, we performed the same analysis for one neutron star (GS 1826–238) and one active galactic nuclei (IC 4329A) for comparison. No clear differences are found among the three category sources, suggesting that the accretion mechanisms in the low/hard states are independent of mass of the central objects.

VI Microquasar Workshop: Microquasars and Beyond
September 18-22 2006
Società del Casino, Como, Italy

*Speaker.

PoS(MQW6)102

1. Introduction

It is known that Galactic black hole candidates (BHCs) have at least four spectral states: steep power-law state or very high state (intermediate state), thermal-dominant state or high/soft state, low/hard state and quiescent state [1][2]. These states are occured by a change of the accretion disk structure due to the different mass accretion rate. In one of these four states, the low/hard state (hereafter LHS) is frequently observed in the rising and decaying phase of the outburst suggesting a low mass accretion rate. This state is characterized by fast intensity variations with a time scale of $\sim$ msec and its hard X-ray spectrum with a photon index of 1.4–1.7 [1], having a spectral break at $\sim$ 100 keV [3][4]. These high energy emissions are generally accepted to be produced by thermal Comptonization of soft photons in a hot corona such as advection dominated accretion flow (ADAF [5][6]). Some other models such as synchrotron jet emission model [7][8] are present, and its origin is still being debated. High energy radiations with similar spectral shape have been observed in the weak-magnetized neutron star (NS) binaries and active galactic nucleis (AGNs) [4][9]. Their high energy cutoffs are also present around 100 keV, so common emission mechanisms might work in the different mass system over 1.4 to 10^6–10^9 solar mass. However, the best-studied X-ray energy range in the LHS was 1–20 keV so far, while spectral behavior in the hard X-ray range above 30 keV remains still unknown.

In this paper, we first carried out systematic spectral studies over 2–250 keV range about the LHS of 13 BHCs using large data archives from RXTE and Beppo-SAX observations following GX 339–4 results in Miyakawa et al. (2007)[10]. The main purpose of this study is to clarify emission mechanisms in the LHS throughout detailed study of correlation among photon index, high energy cutoff, and luminosity. Moreover, we analyzed each one sample from NSs and AGNs for comparion with BHCs and report on them.

2. Analysis

For our spectral study, we have used both RXTE and Beppo-SAX data. RXTE carries two pointing instruments: PCA and HEXTE [11], while Beppo-SAX carries four types of narrow-field instruments: LECS, MECS, HPGSPC, and PDS [12]. Both X-ray satellites have advantages in the wide-band spectroscopy with moderate energy resolutions. In these instruments, we used a combination of PCA and HEXTE data for RXTE, and MECS and PDS data for Beppo-SAX so as to cover almost the same energy range of 2–250 keV.

We defined the LHS as the state where 1) the photon index is lower than 2.0 and 2) the enegy spectrum is dominated by a power-law emission based not on timing information such as power spectral density and time lag but only spectral shape. From large archival data sets, we selected in total 343 pointing observations for 11 BHCs, 1 NS and 1 Seyfert Galaxy (AGN) in the LHS. Table 1 shows the list of sources we analyzed in this paper. The list includes 155 observations of GX 339–4 and 55 observations of XTE J1550–564. We analyzed all the data in the standard manner for bright sources using the publicly available software HEASOFT 6.0.2 provided by NASA/GSFC. For the RXTE, the PCA spectrum was taken only from the PCU2 detector which was always turned on during all observations. The 2% systematic errors are added to each PCA spectral bin. The background spectra was constructed using recent background model. The HEXTE spectra were

Table 1: Source list of the black hole candidates used in this study.

Source	Distance	Obs. Number*	Observation Epoch
—Black Hole Candidates—			
GX 339−4	8.0 kpc[13]	152/3	1997 Feb. ∼ 2004 Nov.
XTE J1550−564	5.3 kpc[2]	50/0	1998 Sept. ∼ 2002 Feb.
GRO J1655−40	3.2 kpc[2]	23/0	1998 Aug. ∼ 2005 Oct.
XTE J1118+480	1.8 kpc[2]	18/3	2000 Mar. ∼ 2000 July
XTE J1650−500	4.0 kpc[2]	14/1	2001 Sept. ∼ 2001 Dec.
Cygnus X-1	2.5 kpc[2]	11/4	1996 Mar. ∼ 2000 Nov.
GS 1354−645	10 kpc[14]	8/0	1997 Nov. ∼ 1998 Jan.
XTE J1748−288	8.0 kpc[15]	5/0	1998 July ∼ 1998 Aug.
4U 1630−472	10 kpc[16]	4/0	1998 May
XTE J1859+226	7.6 kpc[17]	3/0	1999 Oct.
H 1743−322	10 kpc[2]	2/0	2003 Mar.
—Neutron Stars—			
GS 1826−238	8.0 kpc[18]	30/6	1997 Apr. ∼ 2000 Sep.
—Seyfert Galaxies—			
IC4329A	z=0.016	0/5	1998 Jan. ∼ 2001 Jan.

* RXTE observation/Beppo-SAX observation.

extracted from cluster A and B. The deadtime correction was made, and background subtraction was performed using the rocking motion data. For the Beppo-SAX, MECS (1, 2, and 3) spectra were accumulated within a circular region of 8' in the X-ray image, around which background spectra were extracted. The PDS background spectra were obtained from the rocking motion. The fitting energy range were 3–20 keV and 18–200 keV for PCA and HEXTE, 1.8–10 keV and 15–250 keV for MECS and PDS, respectively.

The energy spectra from the two instruments, i.e. PCA and HEXTE for the RXTE, and MECS and PDS for the Beppo-SAX, were fitted simultaneously with a power-law with an exponential cutoff. The constant factor is allowed to be free between two instruments. We further modified this continuum with a smeared edge model [19] instead of the reflection component for simplicity. The energy of the edge and width of the edge are fixed at 7.11 keV due to the cold iron K-edge and 10 keV, respectively. Galactic absorption with fixed Galactic hydrogen column density ($N_{\rm H}$) was also added to this model. The value of $N_{\rm H}$ was refered from past soft X-ray observations. After all, we used the spectral models of wabs×cutoffp×smeardge with the four free parameters (a photon index α, a high energy cutoff $E_{\rm cut}$, a normalization factor of cutoffp N, and an edge τ) in the XSPEC. From these spectral fits, we mainly obtained the three parameters: a photon index α, a high energy cutoff $E_{\rm cut}$, and an integrated flux over 2–200 keV (F_{2-200}). We used XSPEC version 12.0 for spectral fitting, and all the statistical error was quoted at 90 %. The flux in the 2–200 keV was converted into the luminosity (L_{2-200}) assuming the distance shown in Table 1.

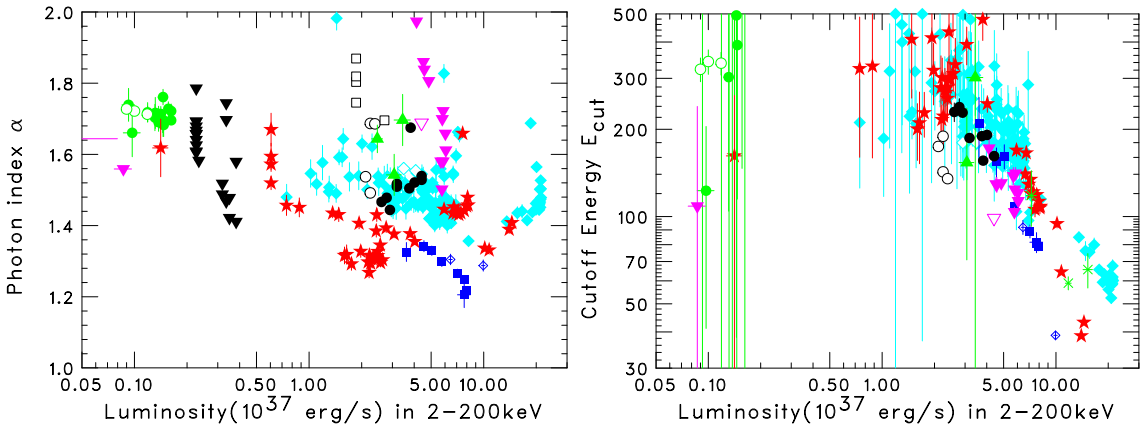

Figure 1: Luminosity dependence of the photon index (α; Left) and the high energy cutoff ($E_{\rm cut}$: Right). GX 339–4 (cyan diamonds), XTE J1550–564 (red stars), GRO J1655–40 (black inverted triangles) and GS 1354–645 (blue squares).

3. Results

3.1 Luminosity Dependence of the Spectral Parameters

Broadband RXTE and Beppo-SAX spectra were succesfully fit by the simple analystic model descrived in the previous section. Figure 1 shows the luminosity (L_{2-200}) dependence of α and $E_{\rm cut}$ for 11 BHCs. The luminosity range was 8×10^{35} to 2×10^{38} erg s^{-1}, corresponding to 0.06–15% of Eddington luminosity with 10 solar mass source. Strictly speaking, L_{2-200} should be normalized to the Eddington luminosity, but the difference of the black hole mass is at most by a factor of 3 [20], so we did not take into account this effect. The α is distributed over 1.2–2.0, while the $E_{\rm cut}$ is more than 30 keV (up to high energy end of the HEXTE and PDS energy coverage).

The first remarkable result is a presence of a clear anti-correlation between L_{2-200} and $E_{\rm cut}$ when L_{2-200} is higher than 2×10^{37} erg s^{-1}, corresponding to about 1–2% of Eddington limit for 10 solar mass BH. The $E_{\rm cut}$ is approximately proportional to L_{2-200}^{-1}. This behavior is already reported in the two different outbursts of GX 339–4 [10]. Similar trend is also reported in another BHC—GRO J0422+22 [6]. This can be explained as due to the more efficient cooling of the energy electron at higher luminosities, which is well explained by ADAF in the quiescent states and low/hard states [6]. Below 2×10^{37} erg s^{-1}, $E_{\rm cut}$ seems to be almost constant at 200–300 keV, but further detailed investigation such as background subtraction will be needed to confirm this fact.

As for the photon index, a weak anti-correlation is found at a luminosity range with less than 2×10^{37} erg s^{-1}. The quiescent state has a softer spectrum with a photon index of 1.8–2.0 than that in LHS [2], hence, the LHS might be smoothly connected to the quiescent state. Above 2×10^{37} erg s^{-1}, the α in some sources get larger rapidly at certain luminosity, which indicates that the state transition from LHS to the steep power-law state may happen around the luminosity.

3.2 Comparison with Weakly-magnetized Neutron Stars and Active Galactic Nuclei

Weakly-magnetized neutron stars and active galactic nuclei are known to have also similar

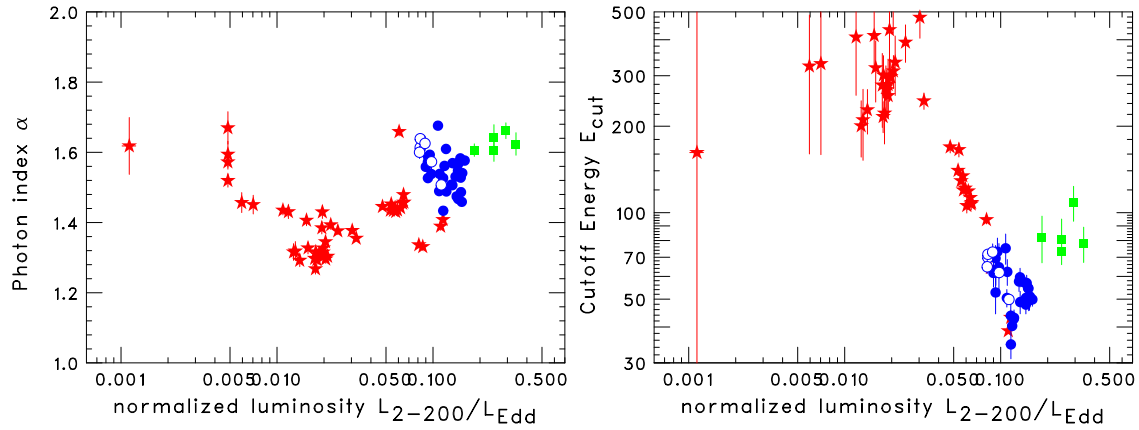

Figure 2: Eddington-scaled luminosity dependence of the photon index (α; Left) and the high energy cutoff ($E_{\rm cut}$: Right) for the three sources: XTE J1550-564 (stars), GS 1826-238 (open and filled stars), and IC 4329A (squares).

energy cutoffs in their energy spectra. In order to find common features in accretion mechanisms, spectral studies were extended to other sources with different mass. We also select the three sources as representatives from each category: XTE J1550−564 for BHCs, GS 1826−238 for NSs and IC 4329A for AGNs. The luminosity L_{2-200} was normalized by the Eddington luminosity ($L_{\rm Edd}$) assuming the mass of the central object as 10 [21], 1.4 and 1.23×10^8 solar mass [22], respectively. The correlation plots are shown in Figure 2. The α is distributed over 1.3–1.7, while the $E_{\rm cut}$ is between 30–300 keV. Suprisingly, the points from GS 1826-238 data were just on the anti-correlation of L_{2-200} and $E_{\rm cut}$ in XTE J1550-564. The points from IC4329A seem to be a bit different from this behavior, but considering that the Eddington ratio of $L_{2-200}/L_{\rm Edd}$ has some uncertainties due to estimations of distance and mass, there may be no significant differences in the three sources. This fact might suggest that the common radiation mechanisms, which are indendent of the central mass, act in NSs and AGNs as well as the LHS of BHCs over a wide mass range of 1–10^9 solar mass.

However, we will need to confirm these important results by collecting much more samples using RXTE data for other BHCs and NSs. Beppo-SAX PDS has a high sensitivity for weak sources, so that we will be able to take more AGN samples. Current INTEGRAL and Suzaku mission will be also powerful for determining an energy cutoff with a higher accuracy.

This research has made use of data obtained through the High Energy Astrophysics Science Archive Research Center Online Service, provided by the NASA/Goddard Space Flight Center.

References

[1] Tanaka, Y., & Shibazaki, N., 1996, ARA&A, 34, 607

[2] McClintok, J.E.,& Remillard, R.E., 2006, in "Compact Stellar X-Ray Sources" eds. W.H.G. Levin and M.V van der Klis, 157

[3] Grove, J.E., Johnson, W.N., Kroeger, R.A., McNaron-Brown, K., Skibo, J.G., Phlips, B.F., 1998, ApJ, 500, 899

[4] Zdziarski, A.A. Poutanen, J., Mikolajewska, J., Gierlinski, M., Ebisawa, K., Johnson, W.N., 1998, MNRAS, 301, 435

[5] Narayan, R., & Yi, I. 1995, ApJ, 452, 710

[6] Esin, A.A., Narayan, R., Cui, W., Grove, J.E., Zhang, S.N., 1998, ApJ, 505, 854

[7] Markoff, S., Falcke, H., & Fender, R., 2001, A&A, 372, L25

[8] Corbel, S., Fender, R.P., Tzioumis, A.K., Nowak, M., McIntyre, V., Durouchoux, P., Sood, R., 2000, A&A, 359, 251

[9] Zdziarski, A.A., Gierlinski, M., Gondek, D., Magdziarz, P., 1996, A&AS, 120, 553

[10] Miyakawa, T.G, Yamaoka, K., Yoshida, A., Saito, K., Dotani, T., Saito, K., Inoue, H., in this volume

[11] Bradt, H.V., Rothschild, R.E., & Swank, J.H. 1993, A&AS, 97, 355

[12] Boella, G., Butler, R. C., Perola, G. C., Piro, L., Scarsi, L., Bleeker, J.A.M., 1997, A&AS, 122, 299

[13] Zdziarski, A.A., Gierlinski, M., Mikolajewska, J., Wardzinski, G., Smith, D.M., Harmon, B.A., Kitamoto, S., 2004, MNRAS, 351, 791

[14] Kitamoto, S., Tsunemi, H., Pedersen, H., Ilovaisky, S.A., van der Klis, M., 1990, ApJ, 361, 590

[15] Hjellming, R.M., Rupen, M.P., Mioduszewski, A.J., Smith, D.A., Harmon, B.A., Waltman, E.B., Ghigo, F.D., Pooley, G.G., 1999, BAAS

[16] Callanan, P.J., McCarthy, J.F., & Garcia, M.R., 2000, A&A, 355, 1049

[17] Hynes, R.I., Haswell, C.A., Chaty, S., Shrader, C.R., Cui, W., 2003, MNRAS, 331, 169

[18] in 't Zand, J.J.M., Heise, J., Kuulkers, E., Bazzano, A., Cocchi, M., Ubertini, P., 1999, A&A, 347, 891

[19] Ebisawa, K., Ogawa, M., Aoki, T., Dotani, T., Takizawa, M., Tanaka, Y., Yoshida, K., Miyamoto, S., Iga, S., Hayashida, K., 1994, PASJ, 46, 375

[20] Orosz, J.A., 2003, Proceedings of IAU Symposium #212, ASP, 365

[21] Orosz, J.A., Groot, P.J., van der Klis, M., McClintock, J. E., Garcia, M.R., Zhao, P., Jain, R.K., Bailyn, C.D. et al., 2002, ApJ, 568, 845

[22] Nikolajuk, M., Papadakis, & I.E., Czerny, B., 2004, MNRAS, 350, L26